Intrinsic Gating Properties of a Cloned G Protein-activated Inward Rectifier K$^+$ Channel

CRAIG A. DOUPNIK, NANCY F. LIM, PAULO KOFUJI, NORMAN DAVIDSON, and HENRY A. LESTER

From the Division of Biology, California Institute of Technology, Pasadena, California 91125

ABSTRACT The voltage-, time-, and K$^+$-dependent properties of a G protein-activated inwardly rectifying K$^+$ channel (GIRK1/KGA/Kir3.1) cloned from rat atrium were studied in *Xenopus* oocytes under two-electrode voltage clamp. During maintained G protein activation and in the presence of high external K$^+$ ($V_K = 0$ mV), voltage jumps from V_K to negative membrane potentials activated inward GIRK1 K$^+$ currents with three distinct time-resolved current components. GIRK1 current activation consisted of an instantaneous component that was followed by two components with time constants $\tau_f \sim 50$ ms and $\tau_s \sim 400$ ms. These activation time constants were weakly voltage dependent, increasing approximately twofold with maximal hyperpolarization from V_K. Voltage-dependent GIRK1 availability, revealed by tail currents at -80 mV after long prepulses, was greatest at potentials negative to V_K and declined to a plateau of approximately half the maximal level at positive voltages. Voltage-dependent GIRK1 availability shifted with V_K and was half maximal at V_K-20 mV; the equivalent gating charge was ~ 1.6 e^-. The voltage-dependent gating parameters of GIRK1 did not significantly differ for G protein activation by three heterologously expressed signaling pathways: m2 muscarinic receptors, serotonin 1A receptors, or G protein $\beta1\gamma2$ subunits. Voltage dependence was also unaffected by agonist concentration. These results indicate that the voltage-dependent gating properties of GIRK1 are not due to extrinsic factors such as agonist-receptor interactions and G protein-channel coupling, but instead are analogous to the intrinsic gating behaviors of other inwardly rectifying K$^+$ channels.

INTRODUCTION

Inwardly rectifying K$^+$ channels (K_{ir} channels) activated by G protein-coupled receptors decrease membrane excitability by hyperpolarizing the membrane potential, slowing membrane depolarization, and shortening the action potential waveform. These tightly regulated K_{ir} channels are functionally expressed in the heart (Kurachi, Tung, Ito, and Nakajima, 1992) and various neurons of the central nervous system (North, 1989), with the best characterized example being the acetyl-

choline (ACh)–activated K_{ir} channel (K_{ACh} channel) expressed in atrial pacemaker cells and myocytes.

Activation of m2 muscarinic receptors on atrial myocytes results in an increase in the probability of K_{ACh} channel opening via a direct membrane-delimited signaling pathway that involves heterotrimeric G proteins (Soejima and Noma, 1984; Breitwieser and Szabo, 1985; Pfaffinger, Martin, Hunter, Nathanson, and Hille, 1985). After the initial controversy over whether pertussis toxin–sensitive $G\alpha$ subunits (Codina, Yatani, Grenet, Brown, and Birnbaumer, 1987; Yatani, Mattera, Codina, Graf, Okabe, Podrell, Iyengar, Brown, and Birnbaumer, 1988) or $G_{\beta\gamma}$ heterodimers (Logothetis, Kurachi, Galper, Neer, and Clapham, 1987; Logothetis, Kim, Northrup, Neer, and Clapham, 1988) mediate the membrane-delimited signaling, it now appears clear that G protein-K_{ACh} channel coupling involves primarily $G_{\beta\gamma}$ dimers (Ito, Tung, Sugimoto, Koboyashi, Takahashi, Katada, Ui, and Kurachi, 1992; Wickman, Inlguez-Lluhl, Davenport, Taussig, Krapivinsky, Linder, Gilman, and Clapham, 1994; Yamada, Ho, Lee, Kontani, Takahashi, Katada, and Kurachi, 1994).

K_{ACh} channel activation by $G_{\beta\gamma}$ subunits represents the primary step in K_{ACh} channel gating. During steady state G protein activation, K_{ACh} channel currents ($I_{K,ACh}$) also display several distinct voltage- and time-dependent gating properties. The foremost of these is inward rectification, mediated by voltage-dependent intracellular Mg^{2+} block (Horie and Irisawa, 1987, 1989) and by voltage-dependent channel gating (Noma and Trautwein, 1978; Sakmann, Noma, and Trautwein, 1983; Iijima, Irisawa, and Kameyama, 1985; Horie and Irisawa, 1987; Simmons and Hartzell, 1987). In response to voltage steps, $I_{K,ACh}$ exhibits relaxations on a time scale of several hundred milliseconds that qualitatively resemble the "intrinsic" voltage-dependent gating processes described for several constitutively active invertebrate (Hagiwara, Miyazaki, and Rosenthal, 1976; Gunning, 1983) and vertebrate (Leech and Stanfield, 1981; Kurachi, 1985; Silver and DeCoursey, 1990) K_{ir} channels. The time-dependent increase in inward K_{ir} current during hyperpolarizing voltage steps from the K^+ equilibrium potential (V_K) is termed "activation," and the time-dependent decrease in outward current during voltage steps positive to V_K is referred to as "deactivation." Constitutively active mammalian K_{ir} currents typically display activation and deactivation on a much faster time scale (<10 ms) than that for $I_{K,ACh}$. Additionally, the gating of constitutively active K_{ir} currents shifts relative to V_K. This property, common among K_{ir} channels, suggests that K^+ binding is an integral step in the gating process (Hille and Schwarz, 1978; Ciani, Krasne, Miyazaki, and Hagiwara, 1978). In this respect, the voltage and K^+ dependence of $I_{K,ACh}$ activation/deactivation has not been fully characterized.

Here we describe the voltage, time, and K^+ dependence of a G protein-activated K_{ir} channel (GIRK1/KGA/Kir3.1) recently cloned from rat atrium (Dascal, Schreibmeyer, Lim, Wang, Chaukin, DiMagno, Labarca, Kieffer, Gaveriaux, Trollinger, Lester, and Davidson, 1993; Kubo, Reuveny, Stesinger, Jan, and Jan, 1993). As in native atrial myocytes, GIRK1 displays slow voltage-dependent activation and steep inward rectification when expressed in *Xenopus* oocytes (Kubo et al., 1993). In the present report, G protein-mediated activation of GIRK1 was initiated in *Xenopus* oocytes by several manipulations involving other coexpressed proteins. The hu-

man m2 receptor and the human serotonin 1A (5-HT$_{1A}$) receptor activated GIRK1 via endogenous oocyte G proteins; and heterologously expressed G protein β1γ2 subunits (G$_{β1γ2}$) activated GIRK1 directly. Our results indicate that the slow voltage-dependent gating of GIRK1 currents represents an intrinsic channel gating process that is independent of the signaling steps leading to channel activation (i.e., ago-nist-receptor coupling and G protein-channel coupling). As for other K_{ir} channels, the voltage dependence of GIRK1 intrinsic gating depends on external K$^+$. The rate constants of GIRK1 activation/deactivation, however, are only weakly voltage dependent in contrast to the steep voltage dependence described for other K_{ir} channels.

The details of I_{KACh} activation and deactivation are interesting as channel gating phenomena but may also be physiologically important. In the heart, these kinetics could determine the shortening of action potential durations and the preservation of intracellular K$^+$ levels during the long plateau phase of the cardiac action potential (Horie and Irisawa, 1987). The voltage-dependent gating properties of these K_{ir} channels may also be important in modulating excitability of central and peripheral neurons (North, 1989). Some of these results were presented in abstract form elsewhere (Doupnik, Lim, Schreibmeyer, Dascal, Davidson, and Lester, 1994a).

MATERIALS AND METHODS

Clones and cRNA

GIRK1 and the human 5-HT$_{1A}$ receptor (provided by P. Hartig, Synaptic Pharmaceuticals Corp.) were cloned in pBluescript II KS (−) (Stratagene, La Jolla, CA). The human m2 receptor (pro-vided by E. Peralta, Harvard University, Cambridge, MA) was cloned in pGEM3Z (Promega Corp., Madison, WI). G$_{β1}$ and G$_{γ2}$ were cloned in pFrogy (provided by A. Connolly and S. Coughlin, Uni-versity of California, San Francisco), a derivative of pCDM8 (Invitrogen Corp., San Diego, CA), in which the G protein gene is flanked by both the 5′ and 3′ untranslated regions of the *Xenopus* β-globin gene. cRNA was transcribed in vitro by T7 or SP6 RNA polymerase (MEGAscript; Am-bion, Austin, TX) from linearized cDNA.

Preparation of Oocytes and cRNA Injection

Immature stage V and VI oocytes from *Xenopus laevis* were enzymatically dissociated from resected ovarian tissue as described elsewhere (Quick and Lester, 1994). Isolated oocytes were maintained at 19°C in a modified Barth's medium of the following composition (in millimolar): 96 NaCl, 2 KCl, 1 CaCl$_2$, 1 MgCl$_2$,5 HEPES (*N*-[2-hydroxyethyl]piperazine-*N*′-[2-ethanesulfonic acid]), 2.5 sodium pyruvate, 0.5 theophylline, 50 μg/ml gentamicin, pH 7.5 (NaOH). The incubation me-dium was changed on a daily basis.

Oocytes were coinjected with 1 ng of GIRK1 cRNA and either 0.5 ng of m2 receptor cRNA, 4 ng of 5-HT$_{1A}$ receptor cRNA, or 1 ng of both G$_{β1}$ and G$_{γ2}$ cRNAs in RNase-free H$_2$O. The final injec-tion volume was 50 nl in all cases. Electrophysiological experiments were performed 4–7 d after injection.

Electrophysiological Recordings

Two-electrode voltage clamping of *Xenopus* oocytes was performed at 19–21°C with an Axoclamp 2A amplifier (Axon Instruments, Inc., Foster City, CA). The voltage recording and current-inject-ing microelectrodes were filled with 3 M KCl and had tip resistances of 0.8–1.2 MΩ. Transmem-

brane potential was measured differentially between the intracellular electrode and a bath electrode in order to minimize series resistance artifacts. The bath electrodes consisted of Ag/AgCl pellets positioned between the oocyte and the suction/output line of the perfusion chamber. Data acquisition and voltage command signals were executed using pCLAMP software (version 5.5.1; Axon Instruments, Inc.) and a microcomputer. Unless otherwise indicated, current signals were low pass filtered at 200 Hz (−3 dB) with an eight-pole Bessel-type filter (Frequency Devices Inc., Haverhill, MA) and digitized at 400 Hz during pCLAMP episodes. The current signal was also continuously recorded on an analogue strip chart recorder. For cumulative dose-response experiments, currents were digitized at 1 Hz and acquired using AxoTape software (Axon Instruments, Inc.). Current analysis and nonlinear curve fitting were performed with pCLAMP and NFITS software (Island Products, Inc., Galveston, TX).

Solutions and Drugs

During electrophysiological recordings, oocytes were continuously superfused with Ca^{2+}-free solutions to reduce the Ca^{2+}-activated Cl^- current ($I_{Cl(Ca)}$) endogenous to *Xenopus* oocytes (Dascal, 1987). Initially, oocytes were superfused with ND98 solution, which consisted of (in millimolar): 98 NaCl, 1 $MgCl_2$, and 5 HEPES, pH 7.5 (NaOH). To record inward K^+ currents, the recording chamber perfusion was switched to a high K^+ (hK) solution that was identical to ND98 with the exception that NaCl was replaced with 98 mM KCl. Rapid activation of heterologously expressed G protein-coupled receptors was accomplished by applying the appropriate receptor agonist in hK solution via a U-tube superfusion apparatus (Bormann, 1992). The exchange rate for the external solution surrounding the oocyte was <1 s, as determined by the time course for ACh activation of heterologously expressed nicotinic ACh receptors (Cohen, Figl, Quick, Labarca, Davidson, and Lester, 1995). A manifold at the input of the U-tube allowed for multiple agonist concentration changes with a minimal delay (~1 s) due to tube dead space.

In several batches of oocytes, ACh superfusion activated $I_{Cl(Ca)}$ presumably by causing intracellular Ca^{2+} release via m2 receptor activation (Lechleiter, Girard, Clapham, and Peralta, 1991) and/or activation of an endogenous muscarinic receptor (see Dascal, 1987). Oocytes were therefore routinely incubated for ~30 min in 100 μM BAPTA/AM (1,2-bis-[o-aminophenoxy]-ethane-N,N,N',N'-tetraacetic acid tetra-[acetoxymethyl]-ester), a membrane-permeant Ca^{2+} chelator. The BAPTA/AM incubation effectively eliminated ACh activation of $I_{Cl(Ca)}$ and reduced the resting membrane conductance of the oocyte.

BAPTA/AM (Calbiochem, San Diego, CA) was made up as a stock concentration of 10 mM dissolved in dimethylsulfoxide and stored in aliquots in darkness at −23°C. ACh and 5-HT (Sigma Chemical Co., St. Louis, MO) were also made up in concentrated stock solutions (in H_2O) that were stored as frozen aliquots at −23°C. All reagents were thawed and used fresh the day of the experiment.

RESULTS

Voltage-Jump Relaxations of GIRK1 Currents

In voltage clamped *Xenopus* oocytes ($V_m = -80$ mV) coexpressing GIRK1 and the m2 receptor, 1 μM ACh activated an inward current ($I_{K,ACh}$) in the presence of high external K^+ (98 mM). The ACh-activated current desensitized partially over a time course of minutes in the continued presence of agonist (Fig. 1 A). Previous studies showed that $I_{K,ACh}$ is highly selective for K^+ ions, exhibits $[Mg^{2+}]_i$-dependent inward rectification, is dependent on receptor activated G proteins, and is sensitive to external Ba^{2+} block (Dascal et al., 1993; Kubo et al., 1993). To study the voltage-

dependent properties of $I_{K,ACh}$, voltage jumps to varying membrane potentials were evoked in high external K^+ in the absence and presence of ACh. $I_{K,ACh}$ was then isolated by digital subtraction of the currents in these two conditions (Fig. 1 *B*). The resulting steady state $I_{K,ACh}(V)$ relation displays (*a*) steep inward rectification and (*b*) a reversal potential (V_{rev}) near the predicted V_K of ~0 mV (Fig. 1 *C*). The lack of
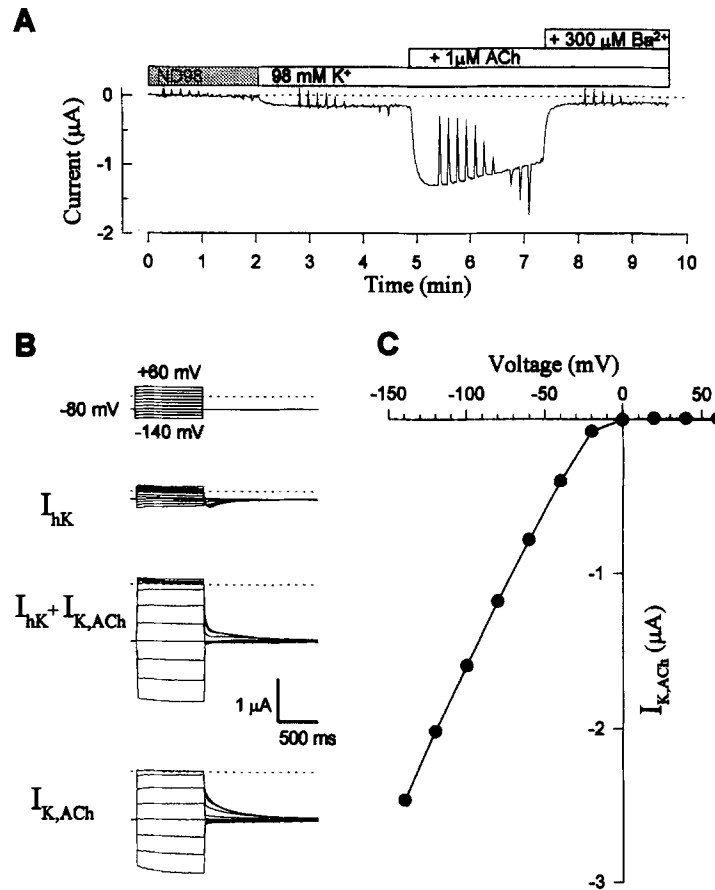

FIGURE 1. Isolation of $I_{K,ACh}$ in a *Xenopus* oocyte coexpressing the m2 receptor and GIRK1. (*A*) Voltage clamp currents at a holding potential of −80 mV. The oocyte was first superfused with a 98 mM K^+ solution, which evoked a small inward current (~100 nA; I_{hK}) caused by both an endogenous K_{ir} current and the agonist-independent activity of GIRK1 (Lim et al., 1994). ACh (1 μM) application evoked a much larger inward $I_{K,ACh}$ (~1.4 μA) that was completely blocked by 300 μM Ba^{2+}. The spikes in the current record are currents evoked by the voltage jumps described in *B*. (*B*) Superimposed currents evoked by 900-ms voltage steps at 0.1 Hz to varying membrane potentials, before (*upper traces*; I_{hK}) and during (*middle traces*; I_{hK} + $I_{K,ACh}$) ACh application. $I_{K,ACh}$ (*lower traces*) was isolated by digital subtraction of the upper traces from the middle traces. (*Dotted line*) Indicates the 0-current level for each family of traces. Capacitive transients have been blanked out. (*C*) Steady state $I_{K,ACh}(V)$ relation. $I_{K,ACh}$ amplitudes were measured isochronally near the end of the voltage step. Note the steep inward rectification of GIRK1 currents expressed in *Xenopus* oocytes.

significant outward I_{KACh} may be attributable to high internal levels of Mg^{2+} (Kubo et al., 1993) or polyamines (Ficker, Taglialatela, Wible, Henley, and Brown, 1994; Lopatin, Makhina, and Nichols, 1994; Fakler, Brandle, Bond, Glowatzki, Koenig, Adelman, Zenner, and Ruppersberg, 1994) that block outward K_{ir} currents. To compensate for I_{KACh} desensitization during the execution of various voltage protocols, each current trace was scaled by a "desensitization factor" calculated by dividing the current amplitude at -80 mV of the first jump in the series by the corresponding current amplitude for each trace. This factor ranged between 1 and 1.35. We found that the degree of desensitization did not affect the I_{KACh} relaxation properties, because very similar time constants were obtained by (a) repeated volt-
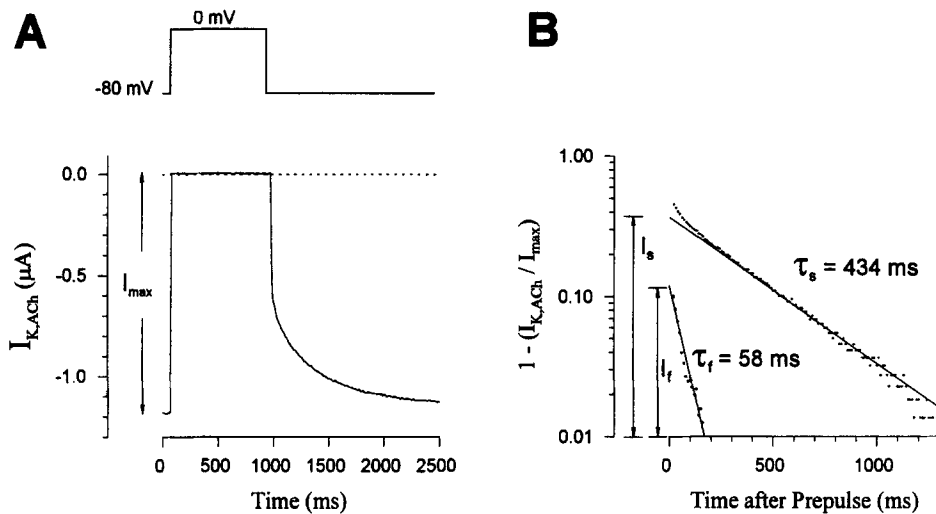

FIGURE 2.   Analysis of voltage-jump relaxation currents for GIRK1. (A) I_{KACh} activation during a hyperpolarizing step to -80 mV after a 900-ms depolarizing prepulse to 0 mV. I_{KACh} was isolated as in Fig. 1 B. (B) Semilogarithmic plot of the I_{KACh} relaxation for the voltage jump from 0 to -80 mV in A. The relaxation was separated into three kinetic components termed instantaneous (I_i), fast (I_f), and slow (I_s), which sum to I_{KACh}. For the fast and slow components, the slope of the line gives the rate constants τ_f^{-1} and τ_s^{-1}, respectively; and extrapolation to the time of the voltage step gives their respective amplitudes.

age jumps at varying times during application of ACh or by (b) reversed voltage pulse sequences.

Time-dependent Kinetics of GIRK1 (Re)activation and Deactivation

Within the time resolution of our voltage clamp circuit ($\sim$5 ms), voltage jumps from a holding potential of -80 mV to positive test potentials resulted in instantaneous changes in I_{KACh}, followed by relatively small outward currents (<100 nA). Similarly, voltage jumps to negative test potentials also resulted in instantaneous changes in I_{KACh}, followed by nearly time-invariant currents. The currents changed

by <10% during the 900-ms voltage steps, although some activation and deactivation could be observed with steps to −140 and −20 mV, respectively (see Fig. 1 B). However, upon repolarization to −80 mV from a positive prepulse potential, $I_{K,ACh}$ reactivated much more slowly. The kinetics of the reactivation were dependent on both prepulse voltage and prepulse duration. Waveforms of $I_{K,ACh}$ activation are shown in Fig. 2 and were described by the following relation:

$$I_{K,ACh}\ (t) = I_i + I_f\exp(-t/\tau_f) + I_s\exp(-t/\tau_s) \tag{1}$$

characterizing three distinct components of GIRK1 activation. After a 900-ms prepulse to 0 mV ($\sim V_K$), $I_{K,ACh}$ reactivation began with an initial instantaneous com-
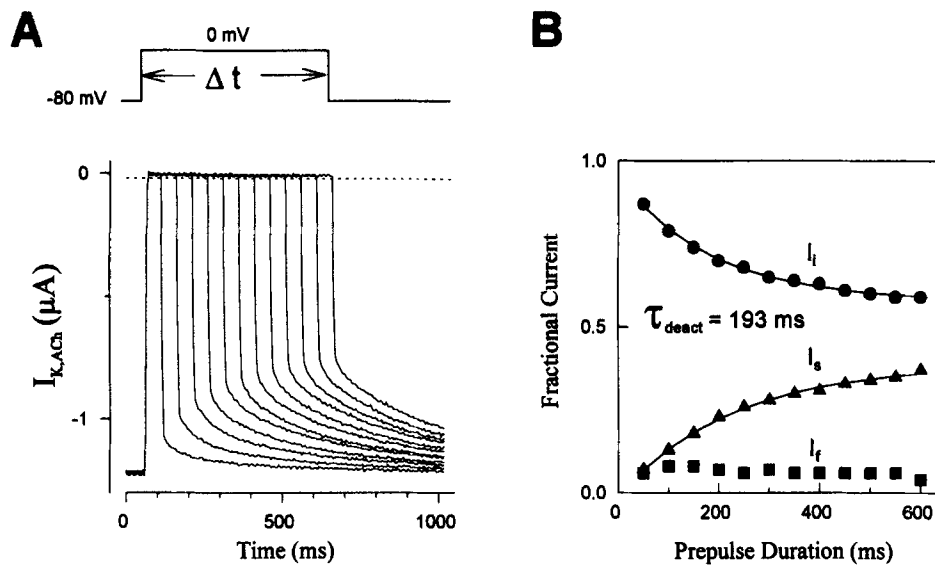

FIGURE 3.   Analysis of $I_{K,ACh}$ deactivation. (A) Effects of prepulse duration on $I_{K,ACh}$ activation kinetics. Depolarizing prepulses to 0 mV were given for varying durations at increments of 50 ms, followed by repolarization to −80 mV. Relaxations during the repolarization were analyzed as in Fig. 2. Episodes were evoked at intervals of 10 s. (B) Fractional amplitudes of I_i (*circles*), I_f (*squares*), and I_s (*triangles*) at −80 mV as a function of the prepulse duration (Δt) at 0 mV. The solid curves through I_i and I_s are single exponential fits to the respective data points with a common time constant (τ_{deact}) of 193 ms.

ponent (I_i) that represented ~50% of the $I_{K,ACh}$ amplitude. The two subsequent components to the voltage-jump relaxations were kinetically resolvable. The faster component (I_f) had a time constant (τ_f) of ~50 ms and comprised ~15% of the current amplitude, and the slower component (I_s) had a time constant (τ_s) of ~400 ms and accounted for ~35% of the $I_{K,ACh}$ amplitude. Prepulse voltage did not affect τ_f or τ_s, but markedly affected I_i, I_f, and I_s (described in the following discussion).

The effects of prepulse duration on the kinetics of $I_{K,ACh}$ activation are shown in Fig. 3. Fig. 3 A demonstrates that after a 50-ms prepulse to 0 mV ($\sim V_K$), $I_{K,ACh}$ reactivation was largely instantaneous with a <10% contribution of I_s. Prepulses of in-

creasing duration increased I_s at the expense of I_f (Fig. 3 B). The time constant of the "envelope current" corresponding to slow channel deactivation (τ_{deact}) was 220 ± 40 ms (mean ± SD, $n = 5$) with prepulses to 0 mV and 242 ± 58 ms ($n = 4$) with prepulses to +20 mV. In one experiment with prepulses to +60 mV, τ_{deact} was 183 ms. Thus, the rate of slow deactivation showed little or no dependence on prepulse potential in the positive voltage range. With prepulses >600 ms in duration, the decrease in I_f approached a plateau at an amplitude ~50% of the total relaxation. Therefore, in the activation studies with 900-ms prepulses (see Fig. 6), channel deactivation was nearly at steady state. In another experiment that achieved steady state deactivation, we set the holding potential to 0 mV rather than
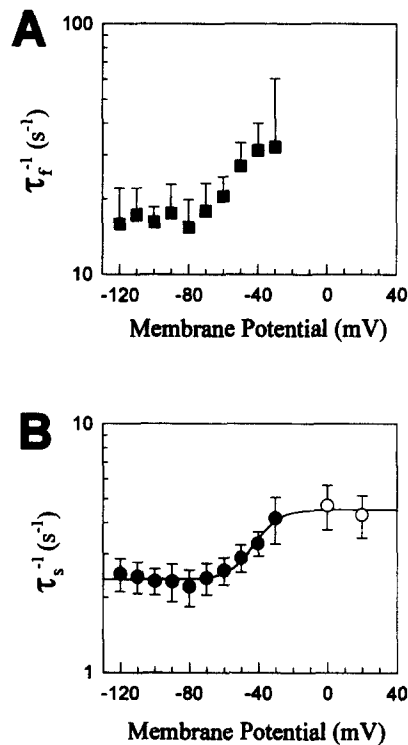

FIGURE 4. Voltage dependence of GIRK1 activation/deactivation. Semilogarithmic plots of (A) τ_f^{-1}, the fast rate constant, and (B) τ_s^{-1}, the slow rate constant (mean ± SD, five oocytes). In B, the closed symbols represent measurements of activation time constants obtained from experiments like that of Fig. 2; the open circles represent the slow deactivation rates from experiments like that of Fig. 3. The solid curve in B is a Boltzmann function fit to the mean data points: τ_s^{-1} (V) = 4.53 − 2.17/{1 + exp[(E_m + 40)/7.4]}.

the usual value of −80 mV and evoked 900-ms test pulses at intervals of 10 s. $I_{K,ACh}$ evoked by hyperpolarizing steps to −80 mV consisted of the three activation components (I_i, I_f, and I_s) in the same fractional ratio (0.50:0.15:0.35, respectively) as reactivation after a 900-ms prepulse to 0 mV.

The amplitude of the fast activation component was unaffected by the prepulse durations tested (Fig. 3 B) and therefore apparently reaches a steady state level of deactivation within the shortest pulse we used (50 ms). We did not systematically study the influence of shorter depolarizing prepulses on the fast component of activation, because this component constitutes a relatively small fraction of the total relaxation amplitude.

Voltage Dependence of GIRK1 Activation/Deactivation Rates

To examine the voltage dependence of τ_f and τ_s, we used a 900-ms depolarizing prepulse to 0 mV; $I_{K,ACh}$ reactivation was then elicited by voltage steps to varying negative test potentials. Fig. 4 shows the rate constants for $I_{K,ACh}$ activation/deactivation (τ_f^{-1} and τ_s^{-1}) as a function of membrane potential. Both τ_f^{-1} and τ_s^{-1} decrease two- to threefold with hyperpolarization between 0 and -80 mV. In contrast to the characteristic steeply voltage-dependent activation/deactivation rate constants of other K_{ir} channels (Kurachi, 1985; Saigusa and Matsuda, 1988; Silver and DeCoursey, 1990), GIRK1 activation/deactivation rates followed a monotonic, sig-
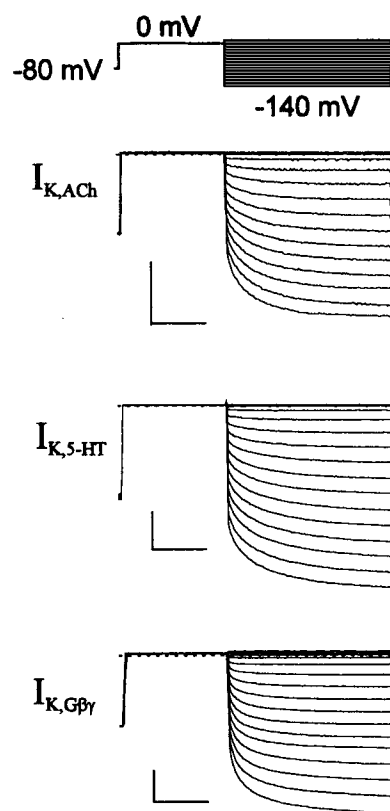

FIGURE 5. Activation of GIRK1 currents during steady state signaling by three different pathways. Traces are from oocytes expressing GIRK1 as well as either m2 receptors ($I_{K,ACh}$), 5-HT$_{1A}$ receptors ($I_{K,5-HT}$), or Gβ1γ2 ($I_{K,G\beta\gamma}$). Voltage was stepped to various levels after a 900-ms depolarizing prepulse to 0 mV. $I_{K,ACh}$ and $I_{K,5-HT}$ were evoked by agonists (1 μM ACh and 100 nM 5-HT, respectively); whereas $I_{K,G\beta\gamma}$ represents currents in high K$^+$ (I_{hK}) minus those in the additional presence of 300 μM Ba^{2+}. Calibration bars denote 0.5 μA and 500 ms.

moidal relation. Although τ_f^{-1} and τ_s^{-1} are weakly voltage dependent over most of the voltage range studied, the $\tau_s^{-1}(V)$ relation displayed a relatively steep transition. In Fig. 4 B, we have fit the data to the sum of a voltage-independent term plus a Boltzmann-type voltage-dependent term having a half-maximal potential at -40 mV and a slope factor of 7.4 mV/e-fold change.

GIRK1 Kinetics Do Not Depend on the G Protein Activation Pathway

We examined the GIRK1 voltage-jump relaxation kinetics for various methods of G protein activation (Fig. 5), including m2 muscarinic receptors, 5-HT$_{1A}$ receptors,

and $G_{\beta1\gamma2}$ expression. After a 900-ms depolarizing prepulse to 0 mV, GIRK1 activation was elicited by voltage steps to varying negative test potentials. For the case of $G_{\beta1\gamma2}$ expression, GIRK1 currents were isolated by subtraction of currents in the presence of 300 μM Ba^{2+}, which blocks all of the GIRK1 current but little of the endogenous hK current (see Fig. 1 A). The voltage-jump relaxation waveforms for the various methods were not significantly different from each other, suggesting that voltage-dependent gating occurs at a point distal to the receptor-G protein activation step.
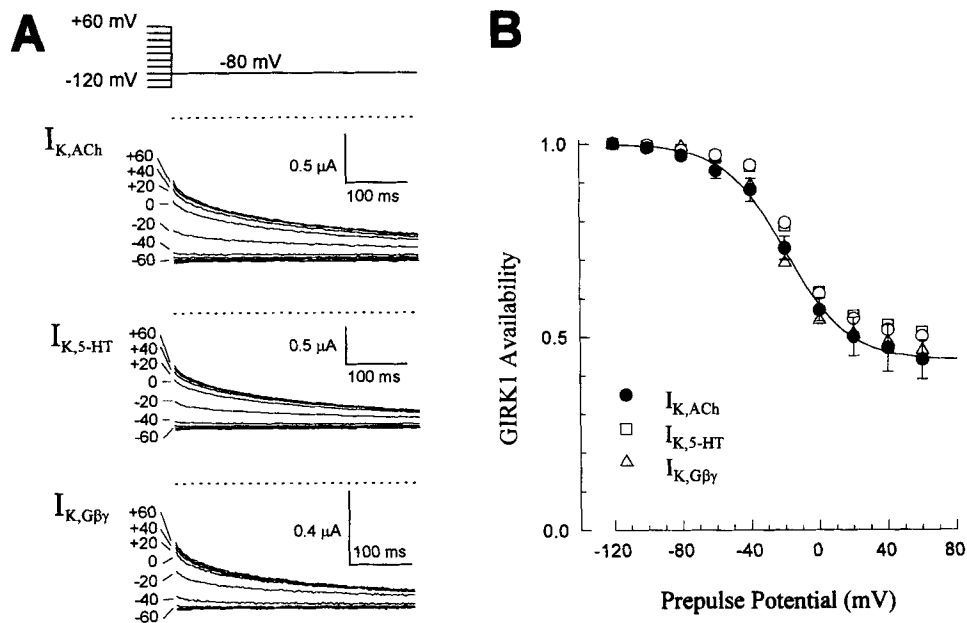

FIGURE 6. Tail current analysis of voltage-dependent GIRK1 availability. (A) GIRK1 tail currents during voltage steps to -80 mV after 900-ms prepulses to varying membrane potentials. GIRK1 was activated either by m2 receptors (*upper traces*), by 5-HT$_{1A}$ receptors (*middle traces*), or by G$\beta1\gamma2$ expression (*lower traces*). The dotted line above each family of tail currents is the 0-current level for the oocyte. (B) Voltage-dependent availability curves for $I_{K,ACh}$ (*open circles*), $I_{K,5-HT}$ (*open squares*), and $I_{K,G\beta\gamma}$ (*open triangles*). Isochronal tail current amplitudes at 10–14 ms after the prepulse step were normalized to the maximal amplitude elicited after prepulses to -120 mV. The solid curve is a Boltzmann function fit to the mean $I_{K,ACh}$ values (*filled circles*, $\pm$SD, six oocytes). The availability curves for $I_{K,5-HT}$ and $I_{K,G\beta\gamma}$ superimpose on that for $I_{K,ACh}$.

Tail Current Analysis of Voltage-dependent GIRK1 Availability

Records like those of Fig. 3 indicate that GIRK1 undergoes time-dependent transitions, namely deactivation, at potentials more positive than V_K. Transitions that occur while no current is flowing were investigated indirectly by experiments that instantaneously reveal channel conducting states. The voltage-dependent availability of GIRK1 was examined by measuring $I_{K,ACh}$ tail current amplitudes after prepulses

that were long enough to achieve steady state activation/deactivation at various membrane potentials.

Fig. 6 shows the relationship between prepulse voltage and normalized tail currents at –80 mV for GIRK1 activated by m2 receptors, by 5-HT$_{1A}$ receptors, or directly via G$_{\beta1\gamma2}$ expression. In each case, the availability of GIRK1 was maximal for prepulses to negative voltages and minimal at voltages near or positive to V_K. The steady state availability relation was well described by the following Boltzmann function:

$$P_o \ (V) = I_{tail}/I_{tail,max} = 1 - (1 - P_{min})/\{1 + \exp[z\delta(V_{1/2} - V_m)/kT]\} \tag{2}$$

where P_o is the relative availability, P_{min} is the minimal plateau value owing to incomplete channel deactivation, $V_{1/2}$ is the potential for half-activation, z is the valence of the charged gating particle, δ is the fractional electrical distance the gating particle moves, k is Boltzmann's constant, and T is the absolute temperature. The product of z and δ, the equivalent gating charge, is given in units of electron charge (e^-). For m2 receptor activation, 5-HT$_{1A}$ receptor activation, and G$_{\beta1\gamma2}$ expression, values for $V_{1/2}$ were -21 ± 4 mV ($n = 13$), -20 ± 4 mV ($n = 7$), and -27 ± 2 mV ($n = 3$), respectively. The equivalent gating charge, corresponding to the slope of the relation, was 1.76 ± 0.25 e^- for m2 receptor activation, 1.64 ± 0.18 $\bar{e}$ for 5-HT$_{1A}$ receptor activation, and 1.62 ± 0.13 e^- for G$_{\beta1\gamma2}$ expression. The P_{min} values, corresponding to the fractional contribution of I_i, were 0.49 ± 0.05 for m2 receptor activation, 0.42 ± 0.05 for 5-HT$_{1A}$ receptor activation, and 0.51 ± 0.03 for G$_{\beta1\gamma2}$ expression. The voltage-dependent reduction in I_i with depolarizing prepulses was accompanied by an increase in both I_f and I_s upon reactivation. In all cases, I_f constituted approximately one third of the deactivated current amplitude and I_s made up approximately two thirds. In summary, the voltage-dependent activation parameters of GIRK1 were not significantly different among the different methods of G protein activation. This result suggests that the voltage-dependent gating occurs at a point distal to the receptor-G protein activation step.

Voltage-dependent Gating of GIRK1 Is Not Due to Voltage-dependent G Protein Coupling

The voltage dependence of GIRK1 activation/reactivation does not depend on the method used to activate G proteins. According to present concepts, both m2 receptor activation and 5-HT$_{1A}$ receptor activation result in the liberation of endogenous G$_{\beta\gamma}$ subunits, which activate GIRK1 by a membrane-delimited pathway. Therefore, results thus far indicate only that GIRK1 kinetics do not distinguish between activation by the heterologously expressed G$_{\beta1\gamma2}$ subunits and endogenous *Xenopus* G$_{\beta\gamma}$ subunits. We therefore asked whether the voltage-dependent activation could reflect voltage-dependent G protein-channel coupling, as proposed for Ca^{2+} channels during G protein-mediated inhibition (see Anwyl, 1991). Currently, there are no direct means to test the voltage dependence of G$_{\beta\gamma}$–GIRK1 interaction. Therefore, the most appropriate tactic was to determine the voltage-dependent activation properties of GIRK1 during various levels of receptor activation. If the dissociation constant for G$_{\beta\gamma}$ coupling to GIRK1 is reduced at positive potentials, which could

account for the reduced GIRK1 availability at positive voltages, the voltage-dependent GIRK1 availability curve would be expected to shift toward more negative membrane potentials at low agonist concentrations ($<EC_{50}$).

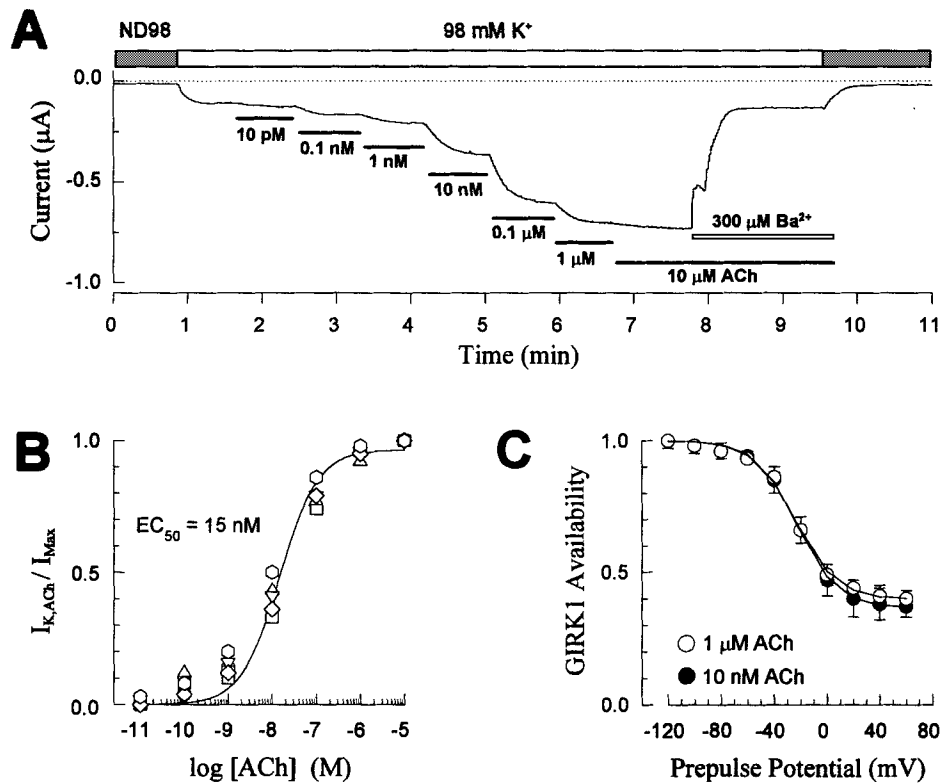Fig. 7 A shows the current trace from a cumulative ACh dose-response experi-

FIGURE 7. Effect of agonist concentration on voltage-dependent $I_{K,ACh}$ availability. (A) Cumulative ACh dose-response experiment for an ooocyte expressing m2 receptors and GIRK1. Increasing concentrations of ACh (solid bars) were superfused via the U-tube apparatus (see Methods). Subsequent bath perfusion with 300 μM Ba^{2+} (open bar) completely blocked the ACh-evoked inward current. The small spike during Ba^{2+} treatment is a bath perfusion artifact resulting from the transition from U-tube superfusion. (B) Normalized ACh dose-response relations from six separate oocytes. The solid curve is a least-squares fit of the data points according to the Hill equation: $I_{K,ACh}/I_{Max} = 1/1 + ([ACh]/EC_{50})$, where the EC_{50} was 15 nM. (C) Voltage-dependent $I_{K,ACh}$ availability during GIRK1 activation by 10 nM (filled circles) and 1 μM (open circles) ACh. Data points are the mean ± SD from four and three oocytes, respectively. (Solid curves) Boltzmann functions fit to the mean data points as described in the text.

ment for GIRK1 activation, and Fig. 7 B shows the normalized dose-response relation. We have fitted the dose-response data to the Hill equation with an EC_{50} of 15 ± 5 nM ($n = 6$) and a Hill coefficient (n_H) of 1.0. The EC_{50} for ACh activation of $I_{K,ACh}$ in atrial cells is ~24 times higher than that for the present data on oocyte ex-

pression (Karschin, Ho, Labarca, Elroy-Stein, Moss, Davidson, and Lester, 1991) and may arise from differences at some point in the transduction pathway for oocytes vs myocytes. Progressive $I_{K,ACh}$ desensitization during the cumulative dose-response protocol may also distort the dose-response relation, although we have not systematically studied this question. For this study, the important point is that the steady state voltage-dependent GIRK1 availability parameters during receptor activation by 10 and 100 nM ACh were indistinguishable from those during activation by 1 μM ACh (Fig. 7C). In addition, the kinetics of voltage-dependent GIRK1 activation were not altered by the level of receptor activation (data not shown). Thus, $G_{\beta\gamma}$ coupling to GIRK1 does not appear to be significantly voltage dependent.

The GIRK1 current relaxations are also not due to a voltage-dependent agonist-receptor interaction. After a rapid change in agonist concentration (<1 s), GIRK1 currents developed with a time constant of ∼8 s (Fig. 8). Therefore, a voltage-dependent agonist-receptor interaction would produce current changes on a time scale of 10–50 s, rather than the 50–500-ms range of the present relaxation experiments.
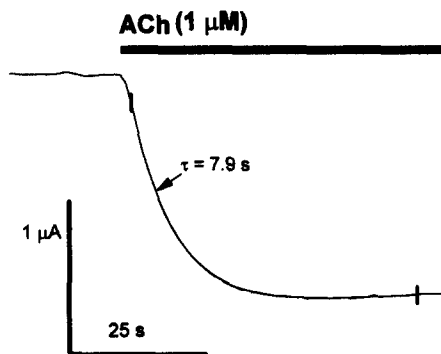
ACh (1 μM)

FIGURE 8. Time course for ACh activation of GIRK1. Rapid application of ACh (1 μM) to an oocyte coexpressing m2 receptors and GIRK1 and voltage clamped at −80 mV. The time course for complete solution change was <1 s. The region of the waveform between the two vertical lines was fitted to a single exponential (time constant, 7.9 s) plus a linearly sloping baseline.

The experiment of Fig. 8 deserves further comment. In most experiments on $I_{K,ACh}$ in atrial myocytes, concentration jumps at the muscarinic receptor lead to conductance relaxations with time constants of ∼300 ms (see, for instance, Nargeot, Lester, Birdsall, Stockton, Wassermann, and Erlander, 1982). The experiment of Fig. 8 shows a much slower time constant, although data for ligand-gated channels expressed in oocytes show that our superperfusion system has a time constant of <1 s (Cohen et al., 1995). We have found that GIRK1 responses to concentration jumps of ACh do become considerably faster for larger m2 receptor cRNA injections. We have not systematically investigated these effects; but the important point is that, under the present conditions, a voltage-dependent agonist–receptor interaction does not explain the relaxations.

K^+-dependent Gating of GIRK1

As for other K_{ir} channels, the voltage-dependent gating properties of GIRK1 were dependent on the external K^+ concentration ($[K^+]_o$), shifting with respect to V_K. Fig. 9 shows the effects of reducing $[K^+]_o$ by fivefold, to 20 mM, on the gating of
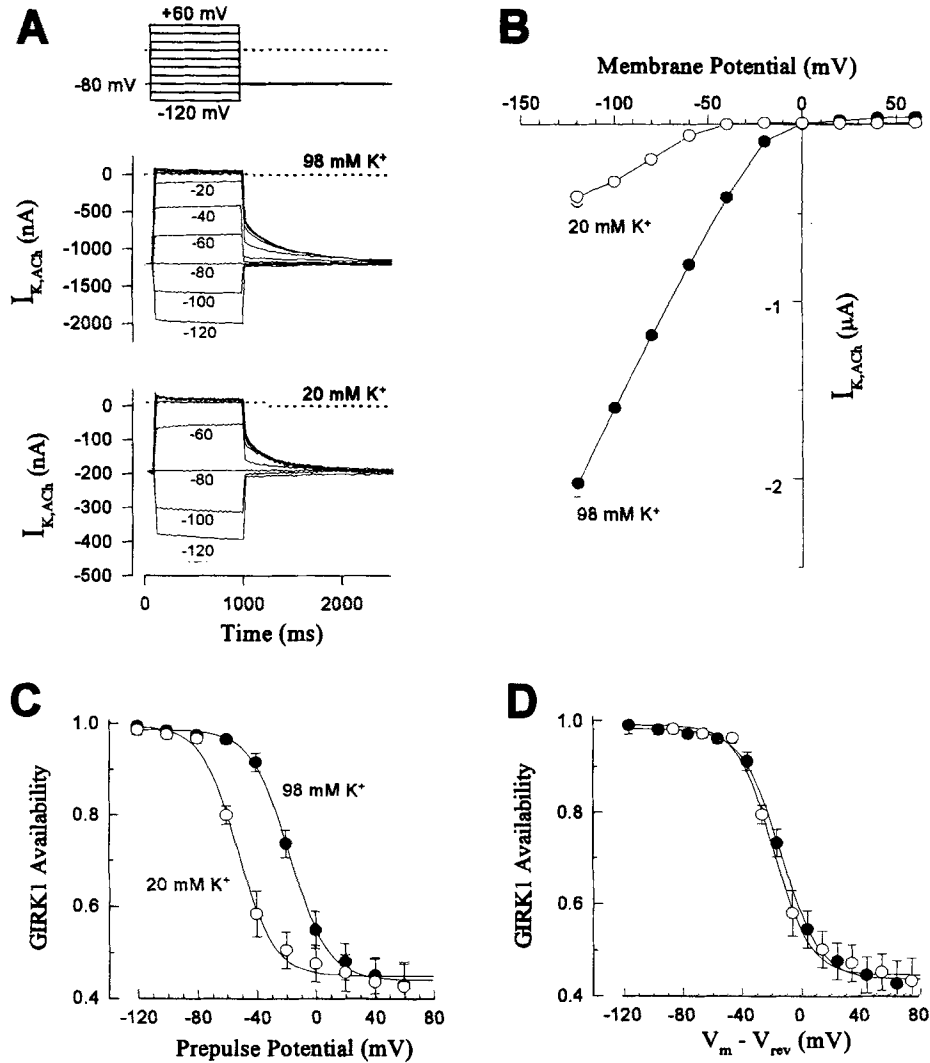
FIGURE 9.   External K$^+$ shifts the voltage dependence of intrinsic GIRK1 gating. (A) $I_{K,ACh}$ during jumps to varying test potentials in 98 mM K$^+$ (*upper traces*) and 20 mM K$^+$ (*lower traces*). (B) Steady state $I_{K,ACh}$ (V) relations in 98 mM K$^+$ (*filled circles*) and 20 mM K$^+$ (*open circles*). V_{rev} for $I_{K,ACh}$ was obtained by interpolation between data points and agreed with the predicted V_K values calculated from the Nernst relation assuming an intracellular K$^+$ concentration of 90 mM. (C) Steady state voltage-dependent GIRK1 availability in 98 mM K$^+$ (*filled circles*) and 20 mM K$^+$ (*open circles*) as determined from tail current measurements (see Fig. 6). The solid curves are Boltzmann functions fit to the mean data values; parameters are described in the text. Data are the mean ± SD ($n = 7$). (D) Steady state GIRK1 availability curves in C after shifting the voltage axis so that it represents $V_m - V_{rev}$.

$I_{K,ACh}$. Isotonic conditions were maintained with either Na^+ or N-methyl-D-gluc-amine substitution. V_{rev} for $I_{K,ACh}$ shifted from 4 ± 6 mV in 98 mM $[K^+]_o$ to -36 ± 5 mV in 20 mM $[K^+]_o$, which is in excellent agreement with the 40-mV shift expected from a fivefold decrease in $[K^+]_o$. Analysis of the voltage-dependent $I_{K,ACh}$ availability relation in 20 mM $[K^+]_o$ yielded a $V_{1/2}$ of -55 ± 3 mV and an equivalent gating charge of 1.90 ± 0.26 e^-. Relative to V_K, the $V_{1/2}$ value in 20 mM $[K^+]_o$ ($V_K - 19$

A

+60 mV

-80 mV

-140 mV

$I_{Rb,ACh}$

0.5 µA

500 ms

B   Membrane Potential (mV)

-150   -100   -50   0   50

-1

-2

$I_{Rb,ACh}$ (µA)

C

1.0

0.5

0.0

-150   -100   -50   0   50

98 mM K^+

98 mM Rb^+
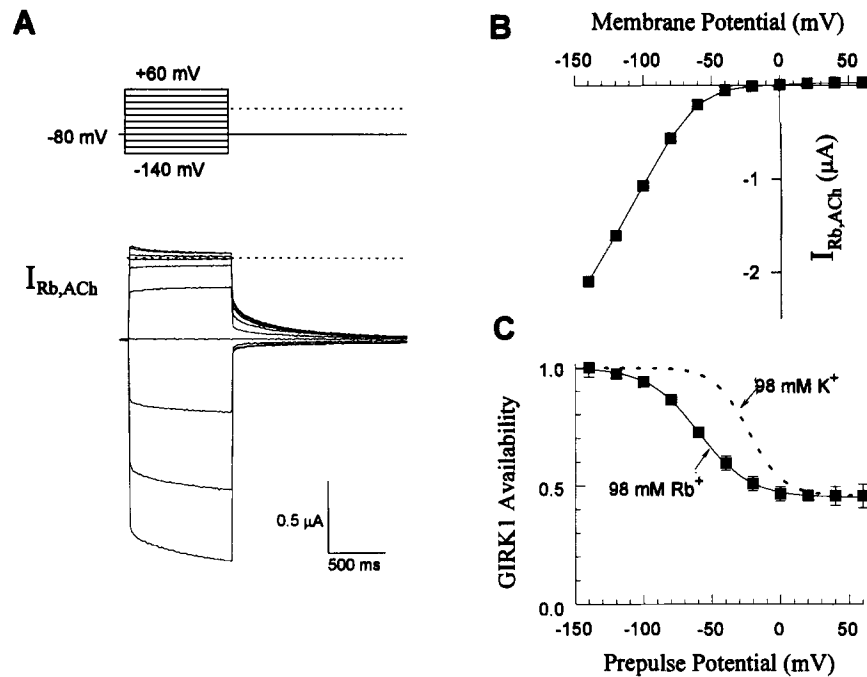
GIRK1 Availability

Prepulse Potential (mV)

FIGURE 10.   Voltage-dependent gating of GIRK1 with Rb^+ as the permeant cation. (*A*) Steady state ACh-activated Rb^+ currents evoked by voltage steps from a holding potential of -80 mV to various membrane potentials between $+60$ and -120 mV. The external Rb^+ concentration was 98 mM. (*B*) Steady state $I_{Rb,ACh}(V)$ relation. $I_{Rb,ACh}$ amplitudes were measured near the end of each voltage step. (*C*) Voltage-dependent $I_{Rb,ACh}$ availability. Normalized $I_{Rb,ACh}$ tail currents were measured isochronally 12 ms after the voltage was jumped to -80 mV after the 900-ms prepulse steps. Data (*filled squares*) are the mean $\pm$ SD from four oocytes. (*Solid curve*) Boltzmann function fit to the mean values as described in the text. For comparison, the broken curve is GIRK1 availability in 98 mM $[K^+]_o$ as shown in Fig. 9 *D*.

mV) was not significantly different from that obtained in 98 mM $[K^+]_o$ ($V_{1/2} = V_K - 21$ mV), nor were the $z\delta$ values (Fig. 9 *D*). Interestingly, the activation rates for GIRK1 activation were not significantly different in 98, 20, or 10 mM $[K^+]_o$, though the weak voltage dependence of τ_s appeared to shift with respect to V_K. These results demonstrate that the voltage-dependent gating of GIRK1 is a function of $[K^+]_o$, which is characteristic of other K_{ir} channels.

To explore the K^+ dependence of gating further, voltage-dependent GIRK1 avail-

ability was examined in the absence of $[K^+]_o$ using 98 mM external Rb^+ as the permeant cation. From the difference in the $I_{Rb,ACh}$ and $I_{K,ACh}$ reversal potentials ($\Delta V_{rev} = V_{Rb,rev} - V_{K,rev} = -8.5 \pm 1.1$ mV), the GIRK1 permeability ratio of Rb^+ to K^+ (P_{Rb}/P_K) was calculated using the following relation from Hille (1992):

$$\Delta V_{rev} = V_{Rb,rev} - V_{K,rev} = (RT/zF) \ln(P_{Rb} [Rb^+]_o/P_K [K^+]_o) \tag{3}$$

where P_{Rb}/P_K was determined to be 0.72 ± 0.03 ($n = 4$). Fig. 10 shows that in 98 mM $[Rb^+]_o$, ACh activated inward Rb^+ currents ($I_{Rb,ACh}$) with characteristic inward rectification and slow activation. Furthermore, the rates of $I_{Rb,ACh}$ activation ($\tau_f = 75 \pm 10$ ms, $\tau_s = 472 \pm 16$ ms) were not significantly different from the rates of $I_{K,ACh}$ activation ($\tau_f = 76 \pm 1$ ms, $\tau_s = 425 \pm 30$ ms) at -80 mV ($n = 4$). The voltage-dependent $I_{Rb,ACh}$ availability curve, however, was significantly shifted to more negative potentials similar to that seen with low $[K^+]_o$; the $V_{1/2}$ value was -60 ± 4 mV. The $V_{1/2}$ value relative to V_{rev} was also significantly more negative (so that $V_{1/2} = V_{rev} -49$ mV) compared with K^+-dependent gating ($V_{1/2} = V_{rev} - 20$ mV). The equivalent gating charge for the $I_{Rb,ACh}$ availability curve ($z\delta = 1.3 \pm 0.3$ e^-) was also significantly less than that for $I_{K,ACh}$. That Rb^+ acts qualitatively like low K^+, shifting both V_{rev} and $V_{1/2}$ to more negative potentials, suggests that external K^+ shifts the voltage dependence of GIRK1 gating positively in a concentration-dependent manner and contributes to or increases the equivalent gating charge of the intrinsic gating mechanism. Rb^+ would substitute only partially for K^+ in these interactions.

DISCUSSION

Slow Activation/Deactivation of GIRK1 Is Analogous to Intrinsic K_{ir} Channel Gating

The results of our study indicate that the voltage-dependent relaxations of GIRK1 currents result from an intrinsic gating process that takes place entirely at the channel protein, rather than from extrinsic factors such as voltage-dependent G protein-channel coupling or agonist-receptor coupling. Evidence supporting this conclusion is as follows. First, three different methods of G protein activation did not alter GIRK1 relaxation properties. GIRK1 activation via m2 receptors, 5-HT$_{1A}$ receptors, and heterologously expressed $G_{\beta1\gamma2}$ subunits produced GIRK1 currents with equivalent voltage-dependent gating kinetics. Second, the level of G protein activation (as controlled by varying the agonist concentration at the G protein-coupled receptor) did not alter the GIRK1 gating kinetics, as predicted if voltage-dependent G protein-GIRK1 coupling mediated the relaxations. Third, external K^+ shifted voltage-dependent GIRK1 gating in a manner characteristic of intrinsic K_{ir} channel gating.

We have used the term "intrinsic" operationally, as has been conventional for describing similar phenomena in other K_{ir} channels. It should be clear, however, that the physical determinants responsible for voltage-dependent GIRK1 gating may indeed be extrinsic to the channel protein itself, in particular K^+ ions (Ciani et al., 1978; Hille and Schwarz, 1978), Mg^{2+} ions (Matsuda, 1991), and/or intracellular polyamines (Ficker et al., 1994; Lopatin et al., 1994; Fakler et al., 1994) interacting

in a voltage-dependent manner with the channel. Our results further support the recent findings that GIRK1 is gated via $G_{\beta\gamma}$ dimers and not by G_{α} subunits (Reuveny, Slesinger, Inglese, Morales, Iniguez-Lluhi, Lefkowitz, Bourne, Jan, and Jan, 1994; Takao, Yoshi, Kanda, Kokubun, and Nukada, 1994; Lim, Dascal, Labarca, Davidson, and Lester, 1995) and therefore support a similar $G_{\beta\gamma}$ coupling mechanism in atrial myocytes (Logothetis et al., 1987; Ito et al., 1992; Wickman et al., 1994; Yamada et al., 1994) as well as in neuronal cells that express GIRK1 (Kubo et al., 1993; Dascal et al., 1993; Karschin, Schreibmeyer, Dascal, Lester, Davidson, and Karschin, 1994). Although our results indicate that the coupling of GIRK1 and $G_{\beta\gamma}$ dimers is not voltage dependent, they do not exclude the potential influence of bound $G_{\beta\gamma}$ dimers in the manifestation of slow channel kinetics.

Comparison of GIRK1 Relaxations with Atrial $I_{K,ACh}$ Relaxations

The voltage-dependent relaxations of GIRK1 agree well with the $I_{K,ACh}$ relaxations previously described in acutely isolated frog atrial myocytes (Simmons and Hartzell, 1987). In frog atrial myocytes, $I_{K,ACh}$ relaxations display an instantaneous component followed by a biexponential time-dependent component with time constants of ~20 and ~300 ms at 21–23°C. The two time constants in frog atrial cells also depend weakly on voltage and follow a sigmoidal relation. Slow $I_{K,ACh}$ relaxations have also been described in guinea pig atrial myocytes (τ range, 50–200 ms at 35–37°C) (Iijima et al., 1985) and rabbit sinoatrial node cells (τ range, 50–150 ms at 35–37°C) (Noma and Trautwein, 1978). Given the high Q_{10} values (>2.5) described for the intrinsic gating of other K_{ir} currents (Leech and Stanfield, 1981; Ishihara et al., 1989), the fast $I_{K,ACh}$ relaxation component identified in frog atrial myocytes and for GIRK1 may have been too fast to resolve at the higher recording temperatures used in the mammalian studies.

Comparison of Intrinsic GIRK1 Gating with Other K_{ir} Channels

Intrinsic gating of GIRK1 and its homologues in native tissue differs from that for other K_{ir} channels in several respects. The first is the presence of three kinetic components in voltage-jump relaxations (I_i, I_f, and I_s) vs two for other K_{ir} channels (I_i and an I_f with a τ <10 ms; see the following discussion). Our interpretation of the three kinetic components for GIRK1 is the presence of three distinct channel closed or blocked states.

Our experiments provide the most complete kinetic data on the slow activation/deactivation component, which we identify with a long channel closed or blocked time. This component is an unusual property of GIRK1 and its apparent homologues in the atria of other species, as has been described. For constitutively active mammalian K_{ir} channels, the reported time constants for activation are typically much faster. For the K_{ir} channel in frog skeletal muscle fibers, τ_{act} is <5 ms at 13°C (Leech and Stanfield, 1981). For the cardiac background K_{ir} channel (i_{K1}), τ_{act} is <5 ms at 30–37°C (Kurachi, 1985; Tourneur, Mitra, Morad, and Rougier, 1987; Harvey and Ten Eick, 1988) and can be slowed down to <10 ms at 14–15°C (Saigusa and Matsuda, 1988; Ishihara et al., 1989) and <20 ms at 8–10°C (Cohen, DiFrancesco, Mulrine, and Pennefather, 1989). For the K_{ir} channel current in bovine pulmonary endothelial cells, τ_{act} is <5 ms at 20–23°C (Silver and DeCoursey, 1990).

Slow rates of activation, however, have been reported for invertebrate K_{ir} currents in starfish (τ_{act} <400 ms at 21–22°C) (Hagiwara, Miyazaki, and Rosenthal, 1976) and *Neanthes* oocytes (τ_{act} <250 ms at 22°C) (Gunning, 1983). The GIRK1 component characterized by τ_s is also unique among vertebrate K_{ir} channels in that it is weakly voltage dependent and shows a sigmoidal $1/\tau_s(V)$ curve (Fig. 4). The only other known K_{ir} channel current displaying a similar sigmoidal $\tau_{act}(V)$ relation is the K_{ir} conductance in oocytes from the marine worm *Neanthes arenaceodentata* (Gunning, 1983).

Similar to other K_{ir} channels, the voltage-dependent availability of GIRK1 is a function of V_K. The value for $V_{1/2}$, relative to V_K, therefore constitutes an appropriate parameter for comparisons of gating among K_{ir} channels. The GIRK1 $V_{1/2}-V_K$ value, −20 mV, is more negative than that for most other K_{ir} channels. For example, the $V_{1/2} - V_K$ value for intrinsic gating of the background cardiac K_{ir} channel is −7 mV (Kurachi, 1985; Saigusa and Matsuda, 1988; Ishihara et al., 1989; Oliva, Cohen, and Pennefather, 1990). For K_{ir} channels in skeletal muscle fibers, the $V_{1/2} - V_K$ value is −25 mV in frog dorsal head semitendinosus muscle (Hestrin, 1981) and −11 mV in frog sartorius muscle (Leech and Standen, 1981). For the endothelial cell K_{ir} channel, the value is −8 mV (Silver and DeCoursey, 1990). In invertebrate cells, the $V_{1/2} - V_K$ value for the K_{ir} conductance in starfish eggs is −16 mV (Hagiwara et al., 1976), and it is +5 mV for the K_{ir} conductance in *Neanthes* oocytes (Gunning, 1983).

For excitable cells, a K_{ir} conductance having a more negative $V_{1/2}-V_K$ value would be more readily shut off during membrane depolarization and action potential firing and thereby may better preserve intracellular K^+ levels (Hille, 1992). For $V_{1/2} - V_K$ values closer to the resting membrane potential, such as the constitutively active K_{ir} channels, channel activity would be more readily increased during locally elevated $[K^+]_o$, causing external K^+ ions to be transported into the cell. This external K^+ "siphoning" or "buffering" role has been proposed for the constitutively active K_{ir} channels in glia (Barres, Chun, and Corey, 1990) and macrophage (McKinney and Gallin, 1988). Such a maintenance role seems less likely for the highly regulated GIRK1.

The effects of Rb^+ on intrinsic K_{ir} channel gating have been examined for i_{K1} in guinea pig ventricular myocytes (Mitra and Morad, 1991) and for the K_{ir} conductance in bovine pulmonary endothelial cells (Silver, Shapiro, and DeCoursey, 1994). In both cases, τ_{act} was increased when Rb^+ was the sole permeant cation versus K^+, whereas with GIRK1 in the present study, neither τ_f nor τ_s was significantly different with Rb^+ as the permeant cation compared with K^+. This difference may be due to the greater voltage dependence of activation exhibited by constitutively active K_{ir} channels. Interestingly, the relation between availability and voltage, as revealed by GIRK1 tail currents, was significantly more negative for $I_{Rb,ACh}$ vs $I_{K,ACh}$. For the K_{ir} currents in endothelial cells, Rb^+ similarly dissociates channel gating from the $V_{1/2}$ − V_{rev} rule; however, $V_{1/2}$ shifts positive to V_{rev} ($V_{1/2} - V_{rev} = +7$ mV, 160 mM $[Rb^+]_o$) compared with the negative displacement in 160 mM $[K^+]_o$ ($V_{1/2} - V_{rev} = -7$ mV). In contrast, for GIRK1, $V_{1/2}$ is shifted further negative from V_{rev} in high Rb^+ ($V_{1/2} - V_{rev} = -49$ mV, 98 mM $[Rb^+]_o$) compared with the already negative displacement from V_{rev} in K^+ ($V_{1/2} - V_{rev} = -20$ mV, 98 mM $[K^+]_o$). These various

differences in the intrinsic gating properties of GIRK1 and other K_{ir} channels may reveal basic mechanistic differences among the K_{ir} channel family.

Implications for Structure-Function Studies

The functional differences between K_{ir} channels and outwardly rectifying voltage-gated K$^+$ channels (K_v channels) were noted long before knowledge of their different molecular structures. The recent cloning of several K_{ir} channels (for review see Doupnik, Davidson, and Lester, 1995) indicates little or no sequence homology with K_v channels with the exception of an $\sim$18 amino acid segment termed the pore region that mediates several pore properties in K_v channels (see Jan and Jan, 1992; Brown, 1993; Pongs, 1993). Members of the K_{ir} channel gene family possess two putative transmembrane (TM) domains per subunit, in contrast to six for each K_v channel subunit. The conserved pore region resides between TM1 and TM2 in K_{ir} channels and between TM5 and TM6 in K_v channels. Because four K_v channel subunits are known to coassemble to form a functional channel, the subunit stoichiometry for K_{ir} channels, although not yet known, is presumed to be four.

Several mechanisms that involve external K$^+$ binding and internal Mg^{2+} block have been proposed to explain the intrinsic gating and inward rectifying properties of K_{ir} channels (Hille and Schwarz, 1978; Ciani et al., 1978; Standen and Stanfield, 1978; Matsuda, 1991; Pennefather, Oliva, and Mulrine, 1992). Now that several cloned K_{ir} channels are available, structure-function studies are beginning to provide new insights into the underlying molecular determinants of K_{ir} channel gating (see Doupnik et al., 1995). Recently, the intrinsic gating of cloned constitutively active K_{ir} channels was found to be controlled by a single residue in TM2 that also affected intracellular block by Mg^{2+} (Stanfield, Davies, Shelton, Sutcliffe, Khan, Brammer, and Conley, 1994; Lu and MacKinnon, 1994; Wible, Taglialatela, Ficker, and Brown, 1994) and polyamines (Ficker et al., 1994; Lopatin et al., 1994; Fakler et al., 1994). These findings provide strong evidence for extrinsic channel block as the mechanism underlying the intrinsic gating phenomenon for these K_{ir} channels. The weak voltage dependence of the slow GIRK1 activation/deactivation rates, however, suggests that other processes may be involved. In preliminary studies, we have indeed identified residues in a different region, the putative pore domain, contributing to the slow intrinsic gating of GIRK1 (Doupnik, Kofuji, Davidson, and Lester, 1994*b*).

REFERENCES

Anwyl, R. 1991. Modulation of vertebrate neuronal calcium channels by transmitters. *Brain Research Reviews.* 16:265–281.

Barres, B. A., L. L. Y. Chun, and D. P. Corey. 1990. Ion channels in vertebrate glia. *Annual Review of*

Neuroscience. 13:441–474.

Bormann, J. 1992. U-tube drug application. *In* Practical Electrophysiological Methods. A Guide for In vitro Studies in Vertebrate Neurobiology. H. Kettenmann and R. Grantyn, editors. Wiley-Liss, New York. 136–140.

Breitwieser, G. E., and G. Szabo. 1985. Uncoupling of cardiac muscarinic and β-adrenergic receptors from ion channels by a guanine nucleotide analogue. *Nature.* 317:538–540.

Brown, A. M. 1993. Functional bases for interpreting amino acid sequences of voltage-dependent K⁺ channels. *Annual Review of Biophysics and Biomolecular Structure.* 22:173–198.

Ciani, S., S. Krasne, S. Miyazaki, and S. Hagiwara. 1978. A model for anomalous rectification: electro-chemical-potential-dependent gating of membrane channels. *Journal of Membrane Biology.* 44:103–134.

Codina, J., A. Yatani, D. Grenet, A. M. Brown, and L. Birnbaumer. 1987. The α subunit of the GTP binding protein Gk opens atrial potassium channels. *Science.* 236:442–445.

Cohen, B. N., A. Figl, M. W. Quick, C. Labarca, N. Davidson, and H. A. Lester. 1995. Regions of β2 and β4 responsible for differences between the steady state dose-response relationships of the α3β2 and α3β4 neuronal nicotinic receptors. *Journal of General Physiology.* In press.

Cohen, I. S., D. DiFrancesco, N. K. Mulrine, and P. Pennefather. 1989. Internal and external K⁺ help gate the inward rectifier. *Biophysical Journal.* 55:197–202.

Dascal, N. 1987. The use of *Xenopus* oocytes for the study of ion channels. *CRC Critical Reviews in Biochemistry.* 22:317–387.

Dascal, N., W. Schreibmayer, N. F. Lim, W. Wang, C. Chavkin, L. DiMagno, C. Labarca, B. L. Kieffer, C. Gaveriaux-Ruff, D. Trollinger, H. A. Lester, and N. Davidson. 1993. Atrial G protein-activated K⁺ channel: expression cloning and molecular properties. *Proceedings of the National Academy of Sciences, USA.* 90:10235–10239.

Doupnik, C. A., N. F. Lim, W. Schreibmayer, N. Dascal, N. Davidson, and H. A. Lester. 1994a. Inactivation and reactivation properties of an atrial G protein-gated K⁺ channel, KGA, expressed in *Xenopus* oocytes. *Biophysical Journal.* 66:A51. (Abstr.)

Doupnik, C. A., P. Kofuji, N. Davidson, and H. A. Lester. 1994b. Pore region residues confer slow voltage-dependent gating of a cloned G protein-activated inward rectifier K⁺ channel. *Society for Neuroscience Abstracts.* 20:362.9. (Abstr.)

Doupnik, C. A., N. Davidson, and H. A. Lester. 1995. The inward rectifier potassium channel family. *Current Opinion in Neurobiology.* 5:268–277.

Fakler, B., U. Brandle, C. Bond, E. Glowatzki, C. Koenig, J. P. Adelman, H. P. Zenner, and J. P. Ruppersberg. 1994. A structural determinant of differential sensitivity of cloned inward rectifier K⁺ channels to intracellular spermine. *Federation of the European Biochemical Society Letters.* 356:199–203.

Ficker, E., M. Taglialatela, B. A. Wible, C. M. Henley, and A. M. Brown. 1994. Spermine and spermidine as gating molecules for inward rectifier K⁺ channels. *Science.* 266:1068–1072.

Gunning, R. 1983. Kinetics of inward rectifier gating in the eggs of the marine polychaete, *Neanthes arenaceodentata. Journal of Physiology.* 342:437–451.

Hagiwara, S., S. Miyazaki, and N. P. Rosenthal. 1976. Potassium current and the effect of cesium on this current during anomalous rectification of the egg cell membrane of a starfish. *Journal of General Physiology.* 67:621–638.

Harvey, R. D., and R. E. Ten Eick. 1988. Characterization of the inward-rectifying potassium current in cat ventricular myocytes. *Journal of General Physiology.* 91:593–615.

Hestrin, S. 1981. The interaction of potassium with the activation of anomalous rectification in frog muscle membrane. *Journal of Physiology.* 317:497–508.

Hille, B. 1992. Ionic Channels of Excitable Membranes. Sinauer Associates, Sunderland, MA.

Hille, B., and W. Schwarz. 1978. Potassium channels as multi-ion single-file pores. *Journal of General*

Physiology. 72:409–442.

Horie, M., and H. Irisawa. 1987. Rectification of muscarinic K⁺ current by magnesium ion in guinea pig atrial cells. *American Journal of Physiology.* 253:H210–H214.

Horie, M., and H. Irisawa. 1989. Dual effects of intracellular magnesium on muscarinic potassium channel current in single guinea-pig atrial cells. *Journal of Physiology.* 408:313–332.

Iijima, T., H. Irisawa, and M. Kameyama. 1985. Membrane currents and their modification by acetylcholine in isolated single atrial cells of the guinea-pig. *Journal of Physiology.* 359:485–501.

Ishihara, K., T. Mitsuiye, A. Noma, and M. Takano. 1989. The Mg²⁺ block and intrinsic gating underlying inward rectification of the K⁺ current in guinea-pig cardiac myocytes. *Journal of Physiology.* 419:297–320.

Ito, H., R. T. Tung, T. Sugimoto, I. Koboyashi, K. Takahashi, T. Katada, M. Ui, and Y. Kurachi. 1992. On the mechanism of G protein βγ subunit activation of the muscarinic K⁺ channel in guinea pig atrial cell membrane: comparison with the ATP-sensitive K⁺ channel. *Journal of General Physiology.* 99:961–983.

Jan, L. Y., and Y. N. Jan. 1992. Structural elements involved in specific K⁺ channel functions. *Annual Review of Physiology.* 54:537–555.

Karschin, A., B. Y. Ho, C. Labarca, O. Elroy-Stein, B. Moss, N. Davidson, and H. A. Lester. 1991. Heterologously expressed serotonin 1A receptors couple to muscarinic K⁺ channels in heart. *Proceedings of the National Academy of Sciences, USA.* 88:5694–5698.

Karschin, C., W. Schreibmayer, N. Dascal, H. Lester, N. Davidson, and A. Karschin. 1994. Distribution and localization of a G protein-coupled inwardly rectifying K⁺ channel in the rat. *Federation of the European Biochemical Society Letters.* 348:139–144.

Kubo, Y., E. Reuveny, P. A. Slesinger, Y. N. Jan, and L. Y. Jan. 1993. Primary structure and functional expression of a rat G-protein-coupled muscarinic potassium channel. *Nature.* 364:802–806.

Kurachi, Y. 1985. Voltage-dependent activation of the inward-rectifier potassium channel in the ventricular cell membrane of guinea-pig heart. *Journal of Physiology.* 366:365–385.

Kurachi, Y., R. T. Tung, H. Ito, and T. Nakajima. 1992. G protein activation of cardiac muscarinic K channels. *Progress in Neurobiology.* 39:229–246.

Lechleiter, J., S. Girard, D. Clapham, and E. Peralta. 1991. Subcellular patterns of calcium release determined by G protein-specific residues of muscarinic receptors. *Nature.* 350:505–508.

Leech, C. A., and P. R. Stanfield. 1981. Inward rectification in frog skeletal muscle fibres and its dependence on membrane potential and external potassium. *Journal of Physiology.* 319:295–309.

Lim, N. F., N. Dascal, C. Labarca, N. Davidson, and H. A. Lester. 1995. A G protein-gated K channel is activated via β2-adrenergic receptors and Gβγ subunits in *Xenopus* oocytes. *Journal of General Physiology.* 105:421–439.

Logothetis, D. E., Y. Kurachi, J. Galper, E. J. Neer, and D. E. Clapham. 1987. The βγ subunits of GTP-binding proteins activate the muscarinic K⁺ channel in heart. *Nature.* 325:321–326.

Logothetis, D. E., D. Kim, J. K. Northup, E. J. Neer, and D. E. Clapham. 1988. Specificity of action of guanine nucleotide-binding regulatory protein subunits on the cardiac muscarinic K⁺ channel. *Proceedings of the National Academy of Sciences, USA.* 85:5814–5818.

Lopatin, A. N., E. N. Makhina, and C. G Nichols. 1994. Potassium channel block by cytoplasmic polyamines as the mechanism of intrinsic rectification. *Nature.* 372:366–369.

Lu, Z., and R. MacKinnon. 1994. Electrostatic tuning of Mg²⁺ affinity in an inward rectifier K⁺ channel. *Nature.* 371:243–246.

Matsuda, H. 1991. Magnesium gating of the inwardly rectifying K⁺ channel. *Annual Review of Physiology.* 53:289–298.

McKinney, L. C., and E. K. Gallin. 1988. Inwardly rectifying whole-cell and single-channel K currents in the murine macrophage cell line J774.1. *Journal of Membrane Biology.* 103:41–53.

Mitra, R. L., and M. Morad. 1991. Permeance of Cs$^+$ and Rb$^+$ through the inwardly rectifying K$^+$ channel in guinea pig ventricular myocytes. *Journal of Membrane Biology.* 122:33–42.

Nargeot, J., H. A. Lester, N. J. M. Birdsall, J. Stockton, N. H. Wassermann, and B. F. Erlanger. 1982. A photoisomerizable muscarinic antagonist. Studies of binding and of conductance relaxations in frog heart. *Journal of General Physiology.* 79:657–678.

Noma, A., and W. Trautwein. 1978. Relaxation of the ACh-induced potassium current in the rabbit sinoatrial node cell. *Pflügers Archiv.* 377:193–200.

North, R. A. 1989. Drug receptors and the inhibition of nerve cells. *British Journal of Pharmacology.* 98: 13–28.

Oliva, C., I. S. Cohen, and P. Pennefather. 1990. The mechanism of rectification of i_{K1} in canine Purkinje myocytes. *Journal of General Physiology.* 96:299–318.

Pennefather, P., C. Oliva, and N. Mulrine. 1992. Origin of the potassium and voltage dependence of the cardiac inwardly rectifying K-current (I_{K1}). *Biophysical Journal.* 61:448–462.

Pfaffinger, P. J., J. M. Martin, D. D. Hunter, N. Nathanson, and B. Hille. 1985. GTP-binding proteins couple cardiac muscarinic receptors to a K channel. *Nature.* 317:536–538.

Pongs, O. 1993. Structure-function studies on the pore of potassium channels. *Journal of Membrane Biology.* 136:1–8.

Quick, M. W., and H. A. Lester. 1994. Methods for expression of excitability proteins in *Xenopus* oocytes. *In* Ion Channels of Excitable Cells. T. Narahashi, editor. Academic Press, Inc., Orlando, FL. 261–279.

Reuveny, E., P. A. Slesinger, J. Inglese, J. M. Morales, J. A. Iniguez-Lluhi, R. J. Lefkowitz, H. R. Bourne, Y. N. Jan, and L. Y. Jan. 1994. Activation of the cloned muscarinic potassium channel by G protein βγ subunits. *Nature.* 370:143–146.

Saigusa, A., and H. Matsuda. 1988. Outward currents through the inwardly rectifying potassium channel of guinea-pig ventricular cells. *Japanese Journal of Physiology.* 38:77–91.

Sakmann, B., A. Noma, and W. Trautwein. 1983. Acetylcholine activation of single muscarinic K$^+$ channels in isolated pacemaker cells of the mammalian heart. *Nature.* 303:250–253.

Standen, N. B., and P. R. Stanfield. 1978. Inward rectification in skeletal muscle: a blocking particle model. *Pflügers Archiv.* 378:173–176.

Stanfield, P. R., N. W. Davies, P. A. Shelton, M. J. Sutcliffe, I. A. Khan, W. J. Brammer, and E. C. Conley. 1994. A single aspartate residue is involved in both intrinsic gating and blockage by Mg^{2+} of the inward rectifier, IRK1. *Journal of Physiology.* 478:1–6.

Silver, M. R., and T. E. DeCoursey. 1990. Intrinsic gating of inward rectifier in bovine pulmonary artery endothelial cells in the presence or absence of internal Mg^{2+}. *Journal of General Physiology.* 96: 109–133.

Silver, M. R., M. S. Shapiro, and T. E. DeCoursey. 1994. Effects of external Rb$^+$ on inward rectifier K$^+$ channels of bovine pulmonary artery endothelial cells. *Journal of General Physiology.* 103:519–548.

Simmons, M. A., and H. C. Hartzell. 1987. A quantitative analysis of the acetylcholine-activated potassium current in single cells from frog atrium. *Pflügers Archiv.* 409:454–461.

Soejima, M., and A. Noma. 1984. Mode of regulation of the ACh-sensitive K channel by the muscarinic receptor in rabbit atrial cells. *Pflügers Archiv.* 400:424–431.

Takao, K., M. Yoshii, A. Kanda, S. Kokubun, and T. Nukada. 1994. A region of the muscarinic-gated atrial K$^+$ channel critical for activation by G protein βγ subunits. *Neuron.* 13:747–755.

Tourneur, Y., R. Mitra, M. Morad, and O. Rougier. 1987. Activation properties of the inward-rectifying potassium channel on mammalian heart cells. *Journal of Membrane Biology.* 97:127–135.

Wible, B. A., M. Taglialatela, E. Ficker, and A. M. Brown. 1994. Gating of inwardly rectifying K$^+$ channels localized to a single negatively charged residue. *Nature.* 371:246–249.

Wickman, K. D., J. A. Inlguez-Lluhl, P. A. Davenport, R. Taussig, G. B. Krapivinsky, M. E. Linder,

A. G. Gilman, and D. E. Clapham. 1994. Recombinant G-protein βγ-subunits activate the muscarinic-gated atrial potassium channel. *Nature.* 368:255–257.

Yamada, M., Y.-K. Ho, R. H. Lee, K. Kontani, K. Takahashi, T. Katada, and Y. Kurachi. 1994. Muscarinic K⁺ channels are activated by βγ subunits and inhibited by the GDP-bound form of α subunit of transducin. *Biochemical and Biophysical Research Communications.* 200:1484–1490.

Yatani, A., R. Mattera, J. Codina, R. Graf, K. Okabe, E. Padrell, R. Iyengar, A. M. Brown, and L. Birnbaumer. 1988. The G protein-gated atrial K⁺ channel is stimulated by three distinct Giα-subunits. *Nature.* 336:680–682.